Tetraalkyl-*p*-urazines and Their Cation Radicals

Stephen F. Nelsen* and Yaesil Kim

S. M. McElvain Laboratories of Organic Chemistry, Department of Chemistry, University of Wisconsin, Madison, Wisconsin 53706

Franz A. Neugebauer, Claus Krieger, and Rolf Siegel

Abteilung Organische Chemie, Max-Planck-Institut für medizinische Forschung, 6900 Heidelberg 1, FRG

Menahem Kaftory†

Department of Chemistry, Technion-Israel Institute of Technology, Technion City, Haifa 32 000, Israel

Received April 16, 1990

X-ray structures for tetramethyl-*p*-urazine **1** and its dithia derivative **3** show these compounds to exist in significantly twisted boat structures with nearly planar nitrogens. The X-ray structure of the fused bicyloco-[2.2.2]octyl derivative cation radical $4^{\bullet+}$ is consistent with a delocalized structure having equivalent N–N bonds and planar nitrogens. ESR and ENDOR data are consistent with delocalized cation radicals in solution. Cyclic voltammetry and cation radical optical absorption data are reported. Differences between the solvent dependence of the optical absorption maximum for $4^{\bullet+}$ and for a bisalkoxyurea which is known to have the positive charge localized ($5^{\bullet+}$) are discussed.

Introduction

Authentic *p*-urazine (tetrahydro-1,2,4,5-tetrazine-3,6-dione) and some alkylated derivatives were first reported by Neugebauer and Fischer in 1982.[1] This work concerns the structural features of the neutral forms and one electron oxidation products of tetramethyl-*p*-urazine **1**, its mono- and dithia analogues **2** and **3**, and the bisbicyclo-[2.2.2]octyl-substituted derivative **4**.

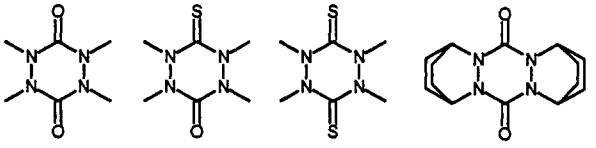

1 **2** **3** **4**

Our interest in **4** and its radical cation was stimulated its structural analogy to bisalkoxyurea **5**.[2] $5^{\bullet+}$ has its

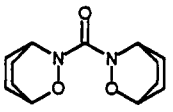

5

positive charge essentially localized on one hydroxylamine unit, and the rate of thermal electron transfer between the hydroxylamine units was measured by variable-temperature ESR. Most significantly, charge transfer bands attributed to vertical electron transfer between the hydroxylamine units were observed in the optical spectrum of $5^{\bullet+}$, allowing application of Marcus–Hush theory to this purely organic radical cation.[2] The relationship between intervalence charge-transfer optical absorption bands and thermal electron-transfer properties of transition metal compounds was developed by Hush[3] and has proven extremely valuable in understanding the electron-transfer properties of these compounds.[4] Analogous purely organic cation radicals had not been studied.[5] Unfortunately, the hydroxylamine subunits of $5^{\bullet+}$ proved not to be satisfactory for these studies because of short lifetimes when the bridge connecting the hydroxylamine subunits was changed, which prevented variation of the distance between the subunits. Although bistetraalkylhydrazines connected by bridges of various lengths have been prepared,[6] optical absorption bands corresponding to electron transfer were not observed,[2] precluding application of Marcus–Hush theory.

We expected that the acylated hydrazine subunits of **4** would confer significantly greater stability on its radical cation than was observed for $5^{\bullet+}$ and hoped that the flattening of the nitrogens induced by having them acylated would allow observation of a charge-transfer band. Furthermore, semiempirical AM1 calculations which work well for electron-transfer considerations in tetraalkylhydrazines predict charge localization on one hydrazine unit for both $1^{\bullet+}$ and $4^{\bullet+}$, which would make these systems very analogous to $5^{\bullet+}$.

Experimental Section

Tetrahydro-1,2,4,5-tetramethyl-1,2,4,5-tetrazine-3,6-dione (1). The mixture of 1,2,4,5-tetrahydro-1,5-dimethyl-1,2,4,5-tetrazine-3,6-dione[7] (2.88 g, 20 mmol), powdered potassium carbonate (15 g), methyl iodide (10 mL), and methanol (10 mL) in acetone (200 mL) was stirred at room temperature for 24 h. The mixture was diluted with diethyl ether (≈100 mL) and filtered, and the residue was washed with diethyl ether. The combined filtrates were evaporated in vacuo. The crude product was dissolved in ethyl acetate and filtered through silica gel to give **1** (2.38 g, 69%): colorless crystals from ethanol–pentane; mp 69–70 °C; IR (CCl_4) 2960 (CH_3), 1680 (CO) cm^{-1}; MS *m/e* 172 (M^+, 100); ^1H NMR ($CDCl_3$, 80 MHz) δ 3.09 (s, 12 H, CH_3). Anal. Calcd for $C_6H_{12}N_4O_2$: C, 41.85; H, 7.02; N, 32.54. Found: C, 41.75; H, 7.06; N, 32.46.

† Work done on sabbatical leave at the California Institute of Technology.

(1) (a) Neugebauer, F. A.; Fischer, H. *Liebigs Ann. Chem.* **1982**, 387. (b) Neugebauer, F. A.; Fischer, H.; Krieger, C. *Tetrahedron Lett.* **1984**, *25*, 629.

(2) Nelsen, S. F.; Thompson-Colon, J. A.; Kaftory, M. *J. Am. Chem. Soc.* **1989**, *111*, 2809.

(3) (a) Hush, N. S. *Trans. Faraday Soc.* **1961**, *575*, 557. (b) Allen, G. C.; Hush, N. S. *Prog. Inorg. Chem.* **1967**, *8*, 357. (c) Hush, N. S. *Ibid.* **1967**, *8*, 391. (d) Hush, N. S. *Electrochim. Acta* **1968**, *13*, 1005. (e) Hush, N. S. *Chem. Phys.* **1975**, *10*, 361.

(4) Creutz, C. *Prog. Inorg. Chem.* **1983**, *30*, 1.

(5) Miller and co-workers are investigating anion radical systems based on quinoines, see: Almlöf, J. E.; Feyereisen, M. W.; Jozefiak, T. H.; Miller, L. L. *J. Am. Chem. Soc.* **1990**, *112*, 1206, and references therein.

(6) Nelsen, S. F.; Willi, M. R.; Mellor, J. M.; Smith, N. M. *J. Org. Chem.* **1986**, *51*, 2081.

(7) Neugebauer, F. A.; Fischer, H.; Siegel. R.; Krieger, C. *Chem. Ber.* **1983**, *116*, 3461.

0022-3263/91/1956-1045$02.50/0

Table I. Crystallographic Data and Refinement Parameters of 1, 3, and $4^{\bullet+}PF_6^-$

	1	3	$4^{\bullet+}PF_6^-$
	$C_6H_{12}N_4O_2$	$C_6H_{12}N_4S_2$	$C_{14}H_{20}N_4O_2PF_6$
formula wt	172.2	204.3	421.3
crystal system	monoclinic	monoclinic	orthorhombic
space group	$P2_1/a$	$P2_1/c$	$Pnn2$
a, Å	11.948 (3)	7.981 (3)	10.629 (5)
b, Å	6.004 (1)	10.809 (4)	9.615 (5)
c, Å	13.522 (3)	11.978 (4)	8.383 (4)
β, deg	113.50 (3)	102.88 (3)	90
V, Å^3	889.6	1007.3	856.7
Z	4	4	2
D_{calcd}, g cm^{-3}	1.29	1.35	1.633
$F(000)$, e	368	432	434
μ(Mo Kα), cm^{-1}	1.10	4.65	1.89
measured reflcns (sin $\theta/\lambda \geq 0.67$ Å^{-1})	2383	2547	
observed reflcns [$I \geq 2\sigma(I)$]	1937	1745	880
R/R_w	0.042/0.040	0.044/0.035	0.080/0.150
max $\Delta\rho$, e Å^{-3}	0.2	0.3	0.4
crystal size, mm^3	0.2 × 0.3 × 0.5	0.1 × 0.1 × 0.3	0.2 × 0.2 × 0.3

Tetrahydro-1,2,4,5-tetramethyl-3-oxo-1,2,4,5-tetrazine-6-thione (2). A suspension of the dione 1 (3.44 g, 20 mmol) and phosphorus pentasulfide (890 mg, 4 mmol) in toluene (550 mL) was stirred and refluxed for 2 h. The mixture was filtered hot, and the solid was extracted twice with bioling toluene. The combined filtrates were dried and concentrated in vacuo. The residue was subjected to column chromatography on silica gel (dichloromethane–ethyl acetate, 4:1). The first fractions gave some tetrahydro-1,2,4,5-tetramethyl-1,2,4,5-tetrazine-3,6-dithione (3) (240 mg, 6%), colorless crystals from ethanol, mp 151–152 °C; R_f (ethyl acetate, DC silica gel 60F) 0.65. The following fractions yielded 2 (1.48 g, 39%): colorless crystals from ethanol–pentane; mp 74–75 °C; R_f 0.4; IR (CCl_4) 2920 (CH_3), 1700 (CO), 1100 (CS) cm^{-1}; MS m/e 188 (M^+, 100); ^{1}H NMR ($CDCL_3$, 80 MHz) δ 3.12 (s, 6 H, 2,4-CH_3), 3.45 (s, 6 H, 1,5-CH_3). Anal. Calcd for $C_6H_{12}N_4OS$: C, 38.28; H, 6.43; N, 29.76; S, 17.03. Found: C, 38.27; H, 6.54; N, 29.71; S, 17.40. Further elution with ethyl acetate gave back starting material (900 mg, 26%, mp 69–70 °C, R_f 0.1).

Tetrahydro-1,2,4,5-tetramethyl-1,2,4,5-tetrazine-3,6-dithione (3). A suspension of 1 (1.72 g, 10 mmol) and phosphorus pentasulfide (8.88 g, 40 mmol) in toluene was stirred and refluxed for 4 h. The reaction mixture was worked up as described above. 3 (1.30 g, 64%): colorless crystals from ethanol; mp 151–152 °C; IR (CCl_4) 2920 (CH_3), 1090 (CS) cm^{-1}; MS m/e 204 (M^+, 100); ^{1}H NMR ($CDCl_3$, 80 MHz) δ 3.44 (s, 12 H, CH_3). Anal. Calcd for $C_6H_{12}N_4S_2$: C, 35.27; H, 5.92; N, 27.42; S, 31.39. Found: C, 34.99; H, 5.96; N, 27.55; S. 31.62.

X-ray Structure Analyses of 1 and 3. The colorless crystals of 1 and 3 were grown from cyclohexane and ethanol, respectively. Intensity data were measured with an Enraf-Nonius CAD-4 four-circle diffractometer with graphite monochromatized Mo$K\alpha$ radiation (λ = 0.71069 Å, $\theta/2\theta$ scanning technique). The intensity data were corrected for the usual Lorentz and polarization effects. The solution of the structures with direct methods and the refinements in full-matrix technique of F^2 were carried out using Multan80[8] and programs of Frenz and Associates.[9] Atomic scattering factors and anomalous-dispersion corrections were taken from ref 10. After anisotropic refinement of the non-hydrogen atoms, all hydrogen atoms were located in the difference Fourier maps and were refined isotropically. The ORTEP drawings were obtained with use of Johnson's program.[11] The crystallographic data and the parameters of structure refinement are given in Table I.

Dodecahydro-1,4:5,8-diethano-9,10-diketo-4a,8a,9a,10a-tetraazaanthracene (4). A solution of free hydrazine was prepared by stirring 0.522 g (2.82 mmol) of 2,3-diazabicyclo-[2.2.2]octane bishydrochloride with 5 g of powdered NaOH in ether under N_2 overnight, followed by filtration through a layer of neutral activated alumina. This solution was added dropwise through a cannula over 40 min to 2.5 g of 12.5% phosgene in toluene, mixed with 1 mL of pyridine, at 0 °C. The mixture was allowed to warm slowly to room temperature and stirred overnight. The mixture was treated with 10 mL of dichloromethane and 10 mL of 1 N HCl in a separatory funnel, and the aqueous layer was extracted with 5 × 15 mL of dichloromethane. The combined organic layers were washed with water and then with 5% sodium bicarbonate until the aqueous layer was neutral, dried with magnesium sulfate, and concentrated to give 110 mg of a yellowish solid 25% crude 4, containing 2,3-diazabicyclo[2.2.2]oct-2-ene. After flash chromatography on alumina eluting with chloroform crystallization from dichloromethane, ether at −20 °C gave 4 as a white crystalline solid, mp >270 °C. Anal. Calcd for $C_{14}H_{20}N_4O_2$: C, 60.83; H, 7.30; N, 20.28. Found: C, 60.81; H, 7.35; N, 20.31. Empirical formula verified by high-resolution mass spectroscopy: calcd for $C_{14}H_{20}N_4O_2$ 276.1586, found 276.1584; ^{1}H NMR ($CDCl_3$) δ 4.26 (br s, 4 H), 2.0–2.15 (m, 8 H), 1.5–1.85 (m, 8 H); ^{13}C NMR ($CDCl_3$) δ 158.22 (CO), 45.79 (CH), 24.75 CH_2); IR ($CDCl_3$) 1655 (C=O) cm^{-1}.

Cation Radical Hexafluorophosphate from 4 ($4^{\bullet+}PF_6^-$). An excess of nitrosyl hexafluorophosphate was added to 80 mg (0.29 mmol) of 4 in 5 mL of methylene chloride and 5 mL of acetonitrile. After the solids dissolved, 30 mL of ether produced a greenish precipitate which was collected and dried under nitrogen to give 108 mg (88%) of blue crude $4^{\bullet+}PF_6^-$, which was recrystallized by vapor diffusion of ether into an acetonitrile solution at −20 °C. This material did not show a clear decomposition point below 200 °C, but the blue color gradually faded upon heating. Anal. Calcd for $C_{14}H_{20}N_4O_2PF_6$: C, 39.89; H, 4.79; N, 13.30. Found: C, 40.00; H, 4.78; N, 13.33.

X-ray Structure Analysis of $4^{\bullet+}PF_6^-$. Blue crystals of $4^{\bullet+}PF_6^-$ crystallized as above were used. Intensity data were measured with an Enraf-Nonius CAD-4 four-circle diffractometer with graphite monochromatized Mo Kα radiation (λ = 0.71069 Å, $\theta/2\theta$ scanning technique). The structure was solved using Multan80.[8] The cation and anion occupy a crystallographic 2-fold axis special position. A total of 124 parameters were refined by minimizing $\sum w(F_o^2 - F_c^2)^2$ with programs of the CRYM system.[12] Atomic scattering factors and anomalous-dispersion corrections were taken from ref 10. R = 0.080 for all 808 independent reflections ($F_o > 0$), S = 2.22 from final converged least-square fit. All non-hydrogen atoms were refined anisotropically, and hydrogens were refined with fixed isotropic vibrational parameters. The vibrational displacement parameters of the fluorine atoms are significantly large, indicating large motions; any attempts to resolve their positions for a disordered model failed. The crystallographic data and the parameters of structural refinement are given in Table I.

Radical Cations. $1^{\bullet+}$–$3^{\bullet+}$ were generated by oxidation of the parent compounds in dichloromethane/trifluoroacetic acid (19:1) with lead tetraacetate at 200 K. ESR spectra were measured with a Varian V-4500 spectrometer; g values were determined by using an AEG NMR gaussmeter and the Hewlett-Packard frequency converter 5246 L (calibration with perylene radical cation). $4^{\bullet+}$ was prepared as detailed above. Its ESR, ENDOR, and triple resonance spectra were measured using a Brucker ESP 300 spectrometer equipped with the ER(ENMR)ENDOR system. Near IR spectra were recorded on a Cary 170 instrument using 1-cm quartz cells. Cyclic voltammetry employed PAR equipment, as previously described.[6]

(8) Main, P.; Fiske, S. J.; Hull, S. E.; Lessinger, L.; Germain, G.; Declercq, J.-P.; Woolfson, M. M. *Mutan80*. A System of Computer Programs for the Automatic Solution of Crystal Structures from X-ray Diffraction Data. Univs. of York, England, and Louvain, Belgium, 1980.

(9) Frenz, B. A. and Associates Inc. *Structure Determination Package*, 4th revised ed.; College station, Tx, and Enraf-Nonius: Delft, The Netherlands, 1982.

(10) *International Tables for X-ray Crystallography*; Kynoch Press: Birmingham, 1974; Vol. IV.

(11) Johnson, C. K. ORTEP-II; Report ORNL-5138, Oak Ridge National Laboratory, Oak Ridge, TN, 1974.

(12) Duchamp, D. J. (1964). CRYM Crystallographic Computing System. Am. Crystallogr. Assoc. Meet., Bozeman, Montana. Paper B14, p 29.

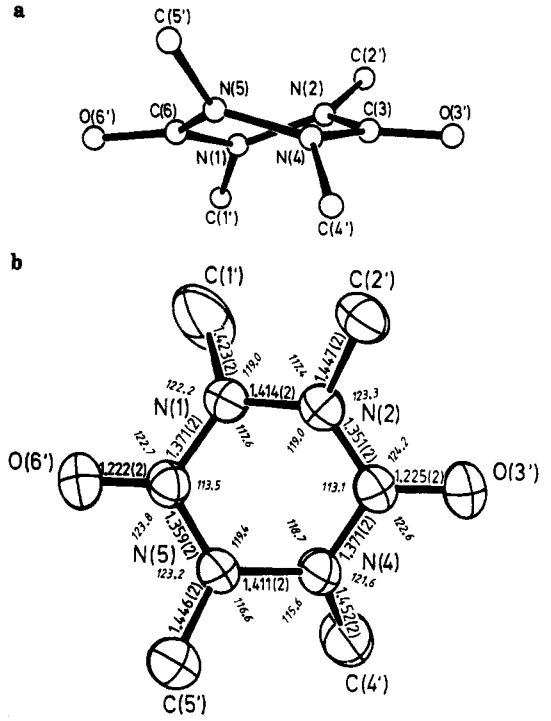

Figure 1. (a) Side view of 1 with the atom numbering; (b) thermal ellipsoid top view plot (50% level) of 1, showing bond lengths (Å) and angles (deg) with their esd's in parentheses.

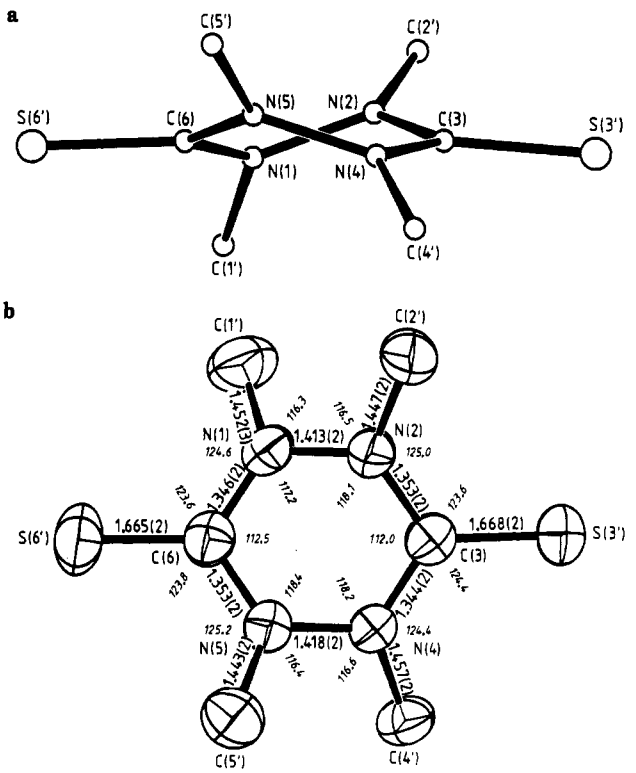

Figure 2. (a) Side view of 3 with the atom numbering; (b) thermal ellipsoid top view view plot (50% level) of 3, showing bond lengths (Å) and angles (deg) with their esd's in parentheses.

Results and Discussion

Crystal Structures of 1 and 3. Views of the molecular structures of 1 and 3 together with atom numbering schemes and bond lengths and angles are shown in Figures 1 and 2. Details of the structure determinations are in the Experimental Section (Table I). The fractional atomic coordinates are summarized in Table II. The rings are in a twist-boat conformation. The torsion angles and the

Table II. Fractional Atomic Coordinates and Equivalent Isotropic Temperature Factors for Non-Hydrogen Atoms of 1 and 3, with Estimated Standard Deviation in Parentheses

$$B_{eq} = \frac{4}{3}\sum_i\sum_j \beta_{ij} a_i \cdot a_j$$

	atom	x	y	z	B_{eq}, Å^2
1	N(1)	−0.0135 (1)	−0.0647 (2)	0.21489 (9)	3.31 (2)
	N(2)	−0.0053 (1)	0.1163 (2)	0.15122 (9)	3.36 (3)
	C(3)	0.1024 (1)	0.2235 (3)	0.17932 (9)	3.20 (3)
	N(4)	0.1732 (1)	0.2138 (3)	0.28775 (9)	4.13 (3)
	N(5)	0.1207 (1)	0.1317 (3)	0.35737 (8)	4.06 (3)
	C(6)	0.0410 (1)	−0.0413 (3)	0.32478 (9)	2.91 (2)
	C(1′)	−0.0551 (4)	−0.2745 (4)	0.1646 (2)	7.49 (9)
	C(2′)	−0.1104 (1)	0.1616 (3)	0.0526 (1)	3.77 (3)
	O(3′)	0.1332 (1)	0.3267 (2)	0.11613 (8)	4.40 (2)
	C(4′)	0.3054 (2)	0.2022 (5)	0.3288 (1)	5.62 (5)
	C(5′)	0.1408 (2)	0.2620 (3)	0.4529 (1)	3.92 (3)
	O(6′)	0.0186 (1)	−0.1642 (2)	0.38661 (8)	4.06 (2)
3	N(1)	0.1822 (2)	0.3920 (2)	0.6681 (2)	3.94 (5)
	N(2)	0.2677 (2)	0.2767 (2)	0.6818 (2)	4.15 (5)
	C(3)	0.2245 (3)	0.1924 (2)	0.5968 (2)	3.21 (6)
	N(4)	0.0603 (2)	0.2047 (2)	0.5394 (2)	3.49 (5)
	N(5)	−0.0504 (2)	0.2802 (2)	0.5878 (2)	3.78 (5)
	C(6)	0.0097 (3)	0.3902 (2)	0.6337 (2)	3.45 (6)
	C(1′)	0.2887 (3)	0.5001 (2)	0.6639 (2)	5.69 (8)
	C(2′)	0.4089 (3)	0.2642 (2)	0.7806 (2)	4.86 (7)
	S(3′)	0.35940 (8)	0.08508 (6)	0.56865 (6)	4.29 (2)
	C(4′)	−0.0062 (3)	0.1620 (2)	0.4225 (2)	4.11 (7)
	C(5′)	−0.2191 (3)	0.2309 (3)	0.5857 (2)	5.36 (8)
	S(6′)	−0.11586 (9)	0.50829 (6)	0.65146 (6)	5.31 (2)

Table III. Distances of Atoms (Å) from the Least-Squares Plane through N(1), N(2), C(3), N(4), N(5), and C(6) for 1 and 3

	1	3
N(1)	0.19	0.22
N(2)	−0.24	−0.26
N(4)	0.18	0.20
N(5)	−0.22	−0.24
C(3)	0.05	0.05
C(6)	0.03	0.04
C(1′)	0.99	1.14
C(2′)	−0.84	−0.91
C(4′)	1.12	0.98
C(5′)	−1.05	−0.99
X(3′)	0.14	0.19
X(6′)	0.10	0.08

Table IV. Torsion Angles (deg) Characterizing the Molecular Twist Conformations for 1 and 3

1	C(1′)N(1)N(2)C(2′)	49.3	C(4′)N(4)N(5)C(5′)	69.9
	C(6)N(1)N(2)C(3)	43.2	C(3)N(4)N(5)C(6)	37.9
	C(2′)N(2)C(3)O(3′)	−18.6	C(5′)N(5)C(6)O(6′)	−32.6
	N(1)N(2)C(3)N(4)	−27.8	N(4)N(5)C(6)N(1)	−22.7
	O(3′)C(3)N(4)C(4′)	−36.7	O(6′)C(6)N(1)C(1′)	−28.5
	N(2)C(3)N(4)N(5)	−10.5	N(5)C(6)N(1)N(2)	−15.2
3	C(1′)N(1)N(2)C(2′)	56.0	C(4′)N(4)N(5)C(5′)	53.9
	C(6)N(1)N(2)C(3)	47.8	C(3)N(4)N(5)C(6)	43.4
	C(2′)N(2)C(3)S(3′)	−20.9	C(5′)N(5)C(6)S(6′)	−23.7
	N(1)N(2)C(3)N(4)	−29.2	N(4)N(5)C(6)N(1)	−25.0
	S(3′)C(3)N(4)C(4′)	−24.1	S(6′)C(6)N(1)C(1′)	−36.3
	N(2)C(3)N(4)N(5)	−13.4	N(5)C(6)N(1)N(2)	−17.2

deviations from the least-squares plane through N(1), N(2), C(3), N(4), N(5), and C(6) (Tables III and IV) show that the structures have an approximate D_2 symmetry. As shown by the thermal parameters the methyl groups in 1 and 3 have a considerable molecular flexibility which is particularly pronounced in the C(1′) group of 1, leading to a significant shortening of the N(1)–C(1′) distance (1.42 Å; atomic coordinates and thermal parameters of the hydrogens at C(1′) were included in the refinement as fixed values). C–N and N–N bond distances are in the expected range. The C=O bond (mean 1.224 Å) of 1 corresponds to an isolated C=O double bond as in aldehydes or ketones

Table V. Fractional Atomic Coordinates and Equivalent Isotropic Temperature Factors for $4^{\bullet+}PF_6^-$

atom	x	y	z	U_{eq}[a] (×10⁴)
P(1)	0	0	0	398 (6)
F(1)	0.1458 (3)	0.0228 (6)	0.0031 (17)	881 (16)
F(2)	−0.0151 (14)	0.1248 (10)	0.1077 (16)	1831 (45)
F(3)	−0.0055 (14)	0.0943 (12)	−0.1475 (12)	1597 (35)
O(1)	1.0180 (14)	0.2747 (4)	0.0516 (18)	529 (15)
N(1)	0.8971 (4)	0.0802 (5)	0.00556 (20)	307 (14)
N(2)	0.8875 (4)	−0.0630 (5)	0.5000 (21)	313 (13)
C(1)	0.7739 (6)	0.1502 (6)	0.5002 (24)	355 (17)
C(2)	0.7052 (14)	0.1096 (17)	0.6481 (24)	540 (51)
C(3)	0.6938 (15)	−0.0520 (18)	0.6459 (21)	473 (41)
C(4)	0.7569 (5)	−0.1132 (6)	0.5009 (25)	373 (17)
C(5)	0.6942 (13)	−0.0608 (17)	0.3456 (20)	427 (27)
C(6)	0.7044 (12)	0.0986 (18)	0.3462 (19)	405 (38)
C(7)	1.0096 (6)	0.1485 (6)	0.5041 (20)	318 (14)

[a] $U_{eq} = {}^1/_3\sum_i\sum_j|U_{ij}(a_i^*a_j^*)(a_i\cdot a_j)|$.

(1.215 Å). This not unusual. Similar values have been observed, for example in 1-methyluracil hydrobromide (1.23 Å),[13a] in 1,3,7,9-tetramethyluric acid (1.21 Å),[13b] etc. The C=S bond (mean 1.667 Å) in **3** is found to be somewhat shorter than S=CR_2 bonds (1.71 Å).

Semiempirical calculations[14] on *p*-urazines underline the problems such calculations continue to have with amides. The 1975 MINDO/3 method optimizes the parent tetra NH compound with ring and nitrogen atoms planar (D_{2h} symmetry), and gets the tetramethyl compound **1** in the experimentally observed twist-boat ring conformation with nearly planar nitrogen atoms (MINDO/3 at D_2 symmetry: OCN,NCO dihedral angle 49.2°, X-ray values 43.2, 37.9°; average of the bond angles at nitrogen, α(av) 119.9°, X-ray values 118.6–119.9°; the deviations of the nitrogens from the plane through the adjacent atoms [e.g. N(1) from the N(2),C(16),C1′) plane] are small, averaging 0.093 Å). However, the newer semiempirical methods get very different shapes for these molecules. MNDO,AM1, and MNDO-PM3 agree in optimizing both the parent and **1** in twist-boat D_2 conformations in preference to planar or chair structures, but the nitrogens are signifiantly pyramidalized (for the optimized D_2 **1**, α(av) is 116.3° by MNDO, 114.5° by AM1,and 114.0° by MNDO-PM3), in contrast to the nearly planar nitrogens present in the X-ray structure of **1**. The substantial differences in both planarity at the nitrogens and in the bond lengths at nitrogen predicted by various semiempirical calculations and observed by X-ray seem to us to preclude using these calculations for detailed understanding of the electronic interactions involved in **1**, and details of these calculations will not be discussed.

Crystal Structure of $4^{\bullet+}$. Compound **4** has bridgehead-fused N,N′-bicyclic substitutents at nitrogen, which force a significantly different *p*-urazine ring conformation from that of **1** by precluding large CN,NC dihedral angles because of the bicyclic rings. We prepared **4** by condensation of 2,3-diazabicyclo[2.2.2]octane with phosgene, as described in the Experimental Section. Several attempts unfortunately did not allow obtaining the X-ray structure of neutral **4**, as we did not succeed in obtaining X-ray quality single crystals.

We chose **4** for investigation because the bicyclic rings are known to give great kinetic stability to cation radicals

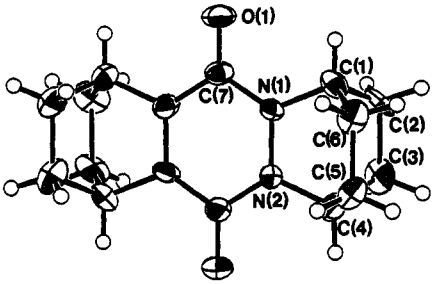

Figure 3. View of $4^{\bullet+}$ with the atom numbering.

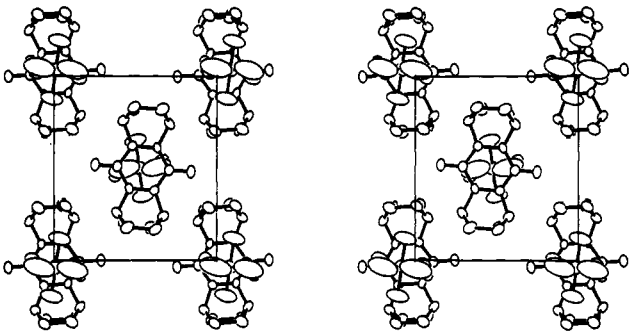

Figure 4. Stereoview of $4^{\bullet+}PF_6^-$ crystal packing.

Table VI. Distances and Bond Angles for $4^{\bullet+}PF_6^-$

	distance (Å)		angle (°)
O(1)-C(7)	1.566 (8)	C(1)-N(1)-N(2)	112.8 (8)
N(1)-N(2)	1.382 (12)	C(7)-N(1)-N(2)	123.0 (8)
N(1)-C(1)	1.473 (14)	C(7)-N(1)-C(1)	124.0 (9)
N(1)-C(7)	1.364 (13)	C(4)-N(2)-N(1)	113.4 (8)
N(2)-C(4)	1.469 (14)	C(7*)-N(2)-N(1)	122.6 (8)
N(2)-C(7*)	1.369 (13)	C(7*)-N(2)-C(4)	123.9 (9)
C(1)-C(2)	1.49 (2)	C(2)-C(1)-N(1)	106.9 (10)
C(1)-C(6)	1.57 (2)	C(6)-C(1)-N(1)	107.4 (9)
C(2)-C(3)	1.56 (2)	C(6)-C(1)-C(2)	111.8 (11)
C(3)-C(4)	1.51 (2)	C(3)-C(2)-C(1)	106.8 (13)
C(4)-C(5)	1.55 (2)	C(4)-C(3)-C(2)	111.3 (13)
C(5)-C(6)	1.54 (2)	C(3)-C(4)-N(2)	107.2 (10)
P(1)-F(1)	1.566 (8)	C(5)-C(4)-N(2)	107.2 (10)
P(1)-F(2)	1.510 (13)	C(5)-C(4)-C(3)	111.1 (11)
P(1)-F(3)	1.534 (12)	C(6)-C(5)-C(4)	107.0 (12)
		C(5)-C(6)-C(1)	110.6 (12)
		N(1)-C(7)-O(1)	123.0 (9)
		N(2*)-C(7)-O(1)	122.7 (9)
		N(2*)-C(7)-N(1)	114.3 (8)
		F(2)-P(1)-F(1)	89.1 (6)
		F(3)-P(1)-F(1)	88.2 (5)
		F(1*)-P(1)-F(1)	178.1 (4)
		F(2*)-P(1)-F(1)	89.8 (6)
		F(3*)-P(1)-F(1)	93.4 (5)
		F(3)-P(1)-F(2)	90.5 (7)
		F(2*)-P(1)-F(2)	106.6 (7)
		F(3*)-P(1)-F(2)	162.8 (7)
		F(3*)-P(1)-F(3)	72.6 (6)

of hydrazines.[15] $NOPF_6$ oxidation of **4** allowed isolation of its cation radical salt. The details of the structure determination of $4^{\bullet+}PF_6^-$ appear in Table I of the Experimental Section, and a stereoview of $4^{\bullet+}$ and the atom numbering scheme are shown in Figures 3 and 4. The fractional atomic coordinates are summarized in Table V, and heavy atom bond lengths and bond angles are given in Table VI. The *p*-urazine ring of $4^{\bullet+}$ is essentially planar, with all dihedral angles under 5° (the largest are C(7)N(1)N(2)C(7a) at 5.0° and C(1)N(1)N(2)C(4) at −4.0°). The N–N distance of $4^{\bullet+}$, at 1.382 (12) Å, is 2.1% shorter

(13) (a) Sobell, H. M.; Tomita, K.-I. *Acta Crystallogr.* **1964**, *17*, 122. (b) Sutor, D. J. *Acta Crystallogr.* **1963**, *16*, 97.

(14) (a) MINDO/3: Bingham, R. C.; Dewar, M. J. H.; Lo, D. H. *J. Am. Chem. Soc.* **1975**, *97*, 1285, 1294, 1302, 1307. (b) MNDO: Dewar, M. J. S.; Thiel, W. *Ibid.* **1977**, *99*, 4489, 4907. (c) AM1: Dewar, M. J. S.; Zoebisch, E. G.; Healy, E. F.; Stewart, J. J. P. *Ibid.* **1985**, *107*, 3902. (d) MNDO-PM3: Stewart, J. J. P. *J. Comput. Chem.* **1989**, *10*, 221.

(15) (a) Nelsen, S. F.; Blackstock, S. C.; Frigo, T. B. *J. Am. Chem. Soc.* **1984**, *106*, 3366. (b) Nelsen, S. F.; Blackstock, S. C.; Haller, K. J. *Tetrahedron* **1986**, *42*, 6101.

Table VII. Isotropic Hyperfine Coupling Constants for $1^{\bullet+}$–$8^{\bullet+}$

	method	a_N(no. of N), G	a_H(no. of nucleus), G	*g* value	lit.
$1^{\bullet+}$	*a*	6.92(4 N)	8.50(12 H)	2.0036	
$2^{\bullet+}$	*a*	6.98(4 N)	8.46(12 H)	2.0036	
$3^{\bullet+}$	*a*	6.96(4 N)	8.43(12 H)	2.0036	
$4^{\bullet+}$	*b*	+6.90(4 N)	+2.06(8 H), −0.31(8 H), +0.06(4 H)	2.0035	
$6^{\bullet+}$	*c*	6.90(4 N)	7.93(12 H), 3.2(2 B)		13
$7^{\bullet+}$	*d*	14.56(2 N)	13.43(6 H), 15.67(4 H)		14
$8^{\bullet+}$	*c*	10.50(2 N)	13.75(6 H), 5.0(^{29}Si)		13
$9^{\bullet+}$	*e*	9.6(2 N)	2.9(4 H)	2.0044	15

[a] Oxidation with lead tetraacetate in dichloromethane–trifluoroacetic acid (19:1) at 213 K. [b] Solution of cation radical salt in dichloromethane–trifluoroacetic acid (19:1); ESR and ENDOR at 240 K. [c] Reaction with $AlCl_3$ in dichloromethane at 225 K. [d] Oxidation with tris(4-bromophenyl)aminium hexachloroantimonate in butyronitrile at room temperature. [e] Oxidation with $NOPF_6$ in dichloromethane at 300 K.

than the average of the N–N distances in **1**, which is considerably less than the 10% N–N bond shortening which has been observed between neutral tetraalkylhydrazines and their cation radicals.[15b] This does not seem too surprising because in contrast to the tetraalkylhydrazine cases, both neutral and oxidized *p*-urazines have planar nitrogens. The positive charge appears to be delocalized over both N–N bonds in $4^{\bullet+}$, although this might be an artifact of disorder. The bond lengths remain unmeasured for neutral **4**, the N–N bond is likely to be significantly longer than of **1** because the nitrogen lone pairs should be at least nearly eclipsed in **4**, while they are at approximately 45° in **1**. If charge were localized on one N–N bond of $4^{\bullet+}$, one would expect a significantly longer N–N bond length and probably pyramidalization at the nitrogens of the unoxidized N–N bond. If this is the case, the packing is completely disordered, and we do not see the elongation of the thermal ellipsoids in the direction of the N–N bonds in Figure 3 that we would expect for this case. The X-ray structure seems most consistent with a delocalized radical cation.

ESR and ENDOR Spectra. ESR spectral data for the radical cations from **1**–**4** are compared with those from model compounds[16–18] **6**–**9** in Table VII, and the ESR spectrum of $1^{\bullet+}$ is shown in Figure 5. In the ENDOR

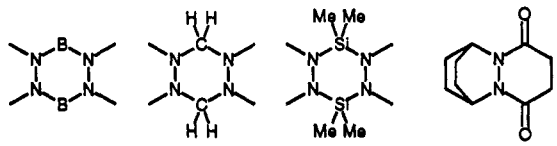

6 **7** **8** **9**

spectrum of $4^{\bullet+}$ (Figure 6a), all ^{1}H and ^{14}N lines were clearly detected and, in addition, by performing general resonance (Figure 6b) relative signs could be determined. Simulation of the highly resolved central part of the ESR spectrum of $4^{\bullet+}$ at 240 K gave best fit with a_N = 6.90 (4 N), a_H = 2.06 (8 H), a_H = 0.32 (8 H), and a_H = 0.06 (4 H) G. As in the similar hydrazide $9^{\bullet+}$ and shown considerably earlier for related semiquinones,[19] we assign the large positive 8 H splitting to the anti (exo) hydrogens, and

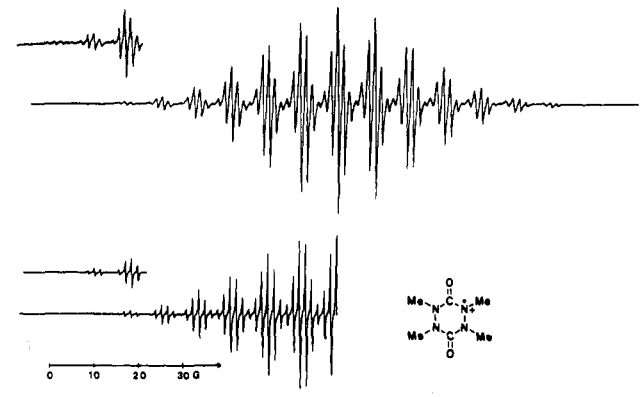

Figure 5. ESR spectrum of $1^{\bullet+}$ in dichloromethane–trifluoroacetic acid (19:1) at 213 K together with a simulation using the data given in Table VII.

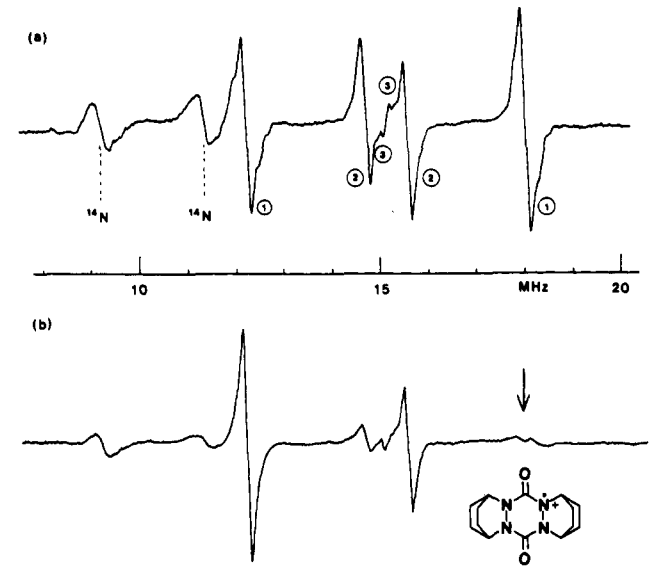

Figure 6. ENDOR (a) and general triple resonance (b) spectra of $4^{\bullet+}$ in dichloromethane–trifluoroacetic acid (19:1) at 240 K.

consequently the small negative 8 H splitting to the syn (endo) hydrogens. $1^{\bullet+}$–$4^{\bullet+}$ and $6^{\bullet+}$ clearly have the "hole" delocalized over both N–N units or are rapidly equilibrating on the ESR time scale, in contrast to the compounds with saturated atoms linking the hydrazine units, $7^{\bullet+}$ and $8^{\bullet+}$, which have the electron localized on one N–N bond on the ESR time scale even at room temperature. Although a(4 N) for $4^{\bullet+}$ is very similar to those for the methylated *p*-urazine derivatives $1^{\bullet+}$–$3^{\bullet+}$, it is 44% larger than is a(2 N)/2 for the mono-diacylhydrazine with the same bicyclic alkyl substituents, $9^{\bullet+}$. The X-ray structure indicates that the nitrogens of $4^{\bullet+}$ are essentially planar at equilibrium, but the larger a(N) value per nitrogen for $4^{\bullet+}$ indicates that pyramidalization at nitrogen of $4^{\bullet+}$ is significantly easier than that of $9^{\bullet+}$.

Optical Spectra and Cyclic Voltammetry Studies. The X-ray structure of $4^{\bullet+}PF_6^-$ is consistent with the "hole" being delocalized over the *p*-urazine ring in the solid, but this would not necessarily be the case in solution. We would expect crystal packing forces to substantially favor the symmetrical, planar *p*-urazine ring structure. We did not see evidence for the ESR spectrum of $4^{\bullet+}$ changing at low temperature as would be expected if this species really had the "hole" instantaneously localized in one hydrazine unit, and electron transfer became slow on the ESR time scale at low temperature. Such effects could already be detected at −30 °C for $5^{\bullet+}$, for which $\Delta G^{\ddagger}$ was determined to be 3.5 kcal/mol.[2] The electron transfer barrier for $4^{\bullet+}$

(16) Bock, H.; Kaim, W.; Semkow, A.; Nöth, H. *Angew. Chem., Int. Ed. Engl.* **1978**, *17*, 286; *Angew. Chem.* **1978**, *90*, 308.
(17) Nelsen, S. F.; Hintz, P. J.; Buschek, J. M.; Weisman, G. R. *J. Am. Chem. Soc.* **1975**, *97*, 4933.
(18) Nelsen, S. F.; Blackstock, S. C.; Rumack, D. T. *J. Am. Chem. Soc.* **1983**, *105*, 3115.
(19) Russell, G. A.; Holland, G. W.; Chang, K.-Y. *J. Am. Chem. Soc.* **1967**, *89*, 6629.

Table VIII. Optical Absorption Maxima for $4^{\bullet+}PF_6^-$ in Various Solvents

solvent	Marcus γ	λ_m, nm	E_{op}, kcal/mol
water	0.550	805	35.52
methanol	0.538	862	33.17
acetonitrile	0.528	862	33.17
ethanol	0.500	873	32.75
$C_4H_6O_3$[a]	0.481	860	33.25
2-propanol	0.474	910	31.42
nitrobenzene	0.384	886	32.27
CH_2Cl_2	0.380	882	32.42
$CHCl_3$	0.268	890	32.13

[a] Propylene carbonate.

must be significantly lower, if the system is not truely delocalized.

We investigated the optical absorption of *p*-urazine cation radicals to try to determine whether or not the "hole" is truly delocalized. The time scale for optical absorption approximates that for light to travel molecular distances, which is far shorter than the ESR time scale, so the problem of fast electron transfer on the ESR time scale making a low barrier for electron transfer appear to be delocalization should not be present. The instanteously charge-localized bisalkoxyurea $5^{\bullet+}$ showed near IR charge transfer absorption with λ_m sensitive to solvent, although this absorption is anomalous in having three maxima (λ_m 1250, 980, and 855 nm in acetonitrile), each band of which is narrower than predicted by Hush theory for a charge transfer band.[2] Nevertheless, the energy of the longest wavelength maximum, E_{op}, gave a linear plot with the Marcus solvent parameter γ, and extrapolation to $\gamma = 0$ gave what was argued to be a reasonable value of λ_{inner} for this compound of 20.5 kcal/mol, suggesting that the near IR absorption observed for $5^{\bullet+}$ actually does correspond to charge transfer between the oxidized and nonoxidized NO bonds. $5^{\bullet+}$ was the first reported organic analogue of a transition-metal intervalence complex, having instanteously localized charge for which a charge-transfer band was observed, making it a Robin-Day[20] Class II species, and allowing application of Hush theory.[3]

Electrolytically generated $1^{\bullet+}ClO_4^-$ and $4^{\bullet+}ClO_4^-$ in dichloromethane show near IR absorption maxima at 910 and 873 nm, respectively. We carried out a solvent study on the position of the band for purified $4^{\bullet+}PF_6^-$ to see if it gives a linear plot with γ, as expected for a Robin-Day Class II complex. The results appear in Table VIII, and plots of the E_{op} versus γ data for $4^{\bullet+}$ and $9^{\bullet+}$ are shown in Figure 7. If only the same five nonhydroxylic solvents which were used in the study of $9^{\bullet+}$ are considered (the circles in Figure 7), reasonable linearity for the E_{op} vs γ plot is seen, although the line is not as good (average vertical deviation from the regression lines shown is 0.08 kcal/mol for $5^{\bullet+}$ and 0.16 kcal/mol for $4^{\bullet+}$). Inclusion of the points for the four hydroxylic solvents (the triangles in Figure 7) destroys the correlation of E_{op} with γ for $4^{\bullet+}$. Even for authentic spin-trapped (Robin-Day Class II) mixed-valence transition-metal complexes, such as Meyer's ligand bridged diruthenium bis(Bipy)chlorides,[21] water has been observed to lie about as much above the line through points determined in nonaqueous solvents in E_{op} vs γ plots as it does for $4^{\bullet+}$.

The near IR optical absorption band for $4^{\bullet+}$ clearly does not, however, pass a second test of Hush theory for this band corresponding to a charge-transfer absorption in a Class II complex. The band is far narrower that it is predicted to be. Transition metal Class II complexes have always had the band width at half-height, $\Delta\bar{\nu}_{1/2}$ (cm^{-1}), larger than the calculated value, $48.06[\bar{\nu}_{max}]^{1/2}$.[4] The values of $\Delta\bar{\nu}_{1/2}$ for $4^{\bullet+}PF_6^-$ in CH_2Cl_2 and CH_3CN are only 355 and 30% % of this value, and the values in methanol, ethanol, and 2-propanol range from 37 to 63% of this value. (Plots of the band in three solvents appear in the supplementary material.) We note, however, that each near IR band for $5^{\bullet+}$ is also considerably narrower than the calculated value,[2] although this species clearly is instantaneously localized because electron transfer between the N–O units becomes slow on the ESR time scale at low temperature.

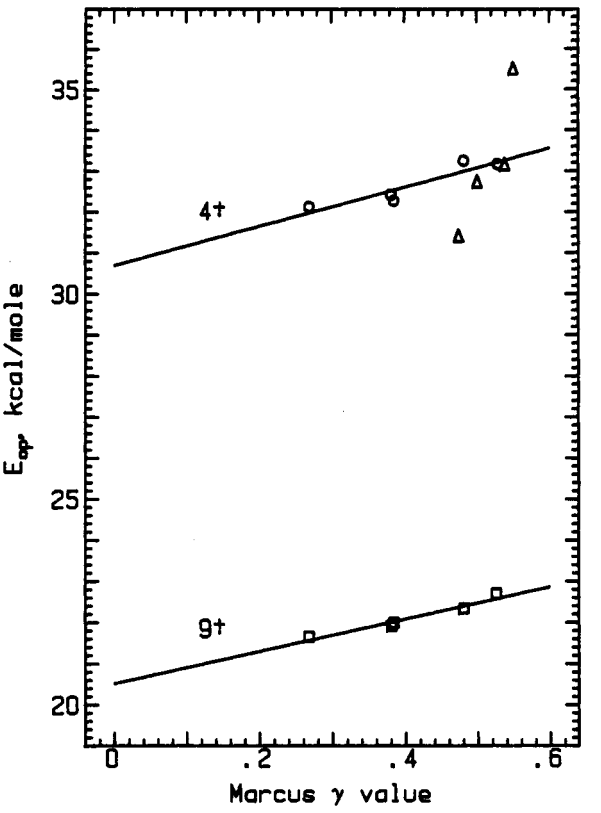

Figure 7. Plot of E_{op} vs γ for $4^{\bullet+}$ and $9^{\bullet+}$.

Table IX. Cyclic Voltammetry Data[a] for *p*-Urazines and Model Compounds

compd	solvent	$E^{\circ\prime}[E_p^{ox} - E_p^{red}]$, V
1	CH_2Cl_2	1.24[0.10]; irrev[b]
2	CH_2Cl_2	irrev, E_p^{ox} 1.34 (0.2 V scan rate)
3	CH_2Cl_2	irrev, E_p^{ox} 1.30 (0.2 V scan rate)
4	CH_2Cl_2	0.92[0.20]; 1.78[0.20]
4	CH_3CN	0.78[0.07]; 1.74[0.07]
9	CH_3CN	1.32[0.07][c]
5	CH_3CN	1.17[0.10][d]
10	CH_3CN	1.15[0.07][e]
11	CH_3CN	1.36[0.07][e]

[a] Conditions: 2 mM substrate in solvent containing 0.1 M tetrabutylammonium perchlorate as supporting electrolite, at Pt, reported vs SCE. [b] E_p^{ox} 1.94 at 0.2 V/s scan rate. [c] From ref 15. [d] From ref 2. [e] From ref 19.

The thermodynamics for electron removal from *p*-urazines and model compounds were studied by cyclic voltammetry (see Table IX). We were unable to observe reversible cv curves **2** and **3**, either at room temperature or −78 °C in dichloromethane, or at room temperature in acetonitrile, at scan rates up to 20 V/s. Failure to observed thermodynamically significant oxidation potentials for

(20) Robin, M. B.; Day, P. *Adv. Inorg. Radiochem.* **1967**, *10*, 247.
(21) (a) Powers, M. J.; Salmon, D. J.; Calahan, R. W.; Meyer, T. J. *J. Am. Chem. Soc.* **1976**, *98*, 6731. (b) Calahan, R. W.; Keene, F. R.; Meyer, T. J. *Ibid.* **1977**, *99*, 1064. (c) Powers, M. J.; Meyer, T. J. *Ibid.* **1980**, *102*, 1289. (d) See also ref 15, footnote 10.

these species precludes significant discussion about the effect of replacing oxygen by sulfur in this work. The much lower $E^{\circ\prime}$ values for **4** than for the monohydrazide **9** is most consistent with $4^{\bullet+}$ being delocalized, but even if $4^{\bullet+}$ were localized, it should be easier to oxidize than **9**. For example, changing from the acetyl substitution of **11** to the (dimethylamino)carbonyl substitution of **10** on the 2-

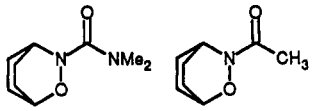

10 **11**

oxa-3-azabicyclo[2.2.2]octyl system lowers $E^{\circ\prime}$ by 0.21 V.[22] The change between **9** and **4**, 0.54 V, is 0.12 V larger than twice the change for C→N substitution at the other side of the carbonyl group in the mononitrogen system, but were are unable to make an accurate estimate of how different $E^{\circ\prime}$ would actually be for producing localized and delocalized $4^{\bullet+}$. For clearly localized radical cations, **5** is no easier to oxidize than its model compound **10**,[2] and **7** is 0.24 V higher in E°, than is *N,N'*-dimethylhexahydropyridazine, which has one pair of NCH_3 units of **7** replaced by CH_2 units.[23]

We suggest that $4^{\bullet+}$ is most likely to be delocalized; it certainly has a significantly lower electron-transfer barrier than does $5^{\bullet+}$ if it is instantaneously localized. This may not have as much to do with the change in 3e-π bonds for bearing the charge from NN to NO as with the differences in geometry restriction in $4^{\bullet+}$ and $5^{\bullet+}$. We pointed out previously that the NO units are not restricted to be syn to each other in $5^{\bullet+}$ (nor anti, as they are in crystalline neutral **5**).[2] Syn geometry is obviously required to be present in $4^{\bullet+}$ by the presence of the two carbonyl bridges between the hydrazine units. An excellent transition-metal analogue for these two situations exists. Powers and Meyer[24] have shown that the monobridged **12**, in which the ferrocene units can assume any orientation between each other is a Robin-Day Class II spin-trapped complex, but its bis-bridged analogue **13** is delocalized.

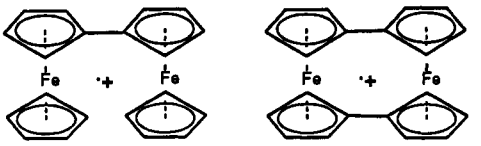

12 **13**

Conclusions

The twist boat conformation of **1** observed by X-ray crystallography is also calculated to be the most stable conformation in the gas phase, but semiempirical calculations do not treat these systems well at all. The X-ray structure of $4^{\bullet+}$ is most consistent with it having a delocalized charge in the solid state. The *p*-urazine cation radicals exhibit spin delocalization over all four nitrogens in solution on the ESR time scale, and from the much sharper near IR absorption peak and the scatter observed in E_{op} vs γ plot for $4^{\bullet+}$, it appears likely that charge is instantaneously delocalized in solution, although the differences between the optical spectral behavior of $4^{\bullet+}$ and that of the clearly localized compound $5^{\bullet+}$ are not great, blurring a firm distinction between true delocalization and instantaneous localization with a very low electron-transfer barrier. The AM1 prediction that $4^{\bullet+}$ would be localized with a significant electron transfer barrier is incorrect, presumably because of the poor treatment of amide bonds by available semiempirical methods.

Acknowledgment. This work was supported by the Deutsche Forschungsgemeinschaft and the National Institutes of Health under Grant GM-29549. M.K. is indebted to Drs. W. P. Schaefer and R. E. Marsh for their hospitality during sabbatical leave at Caltech.

Supplementary Material Available: For **1**, **3**, and $4^{\bullet+}PF_6^-$, lists of atomic coordinates for hydrogen atoms with isotropic temperature factors, anisotropic temperature factors for nonhydrogen atoms, bond distance and angles (**1** and **3**), and torsional angles (**3**); near-IR optical spectra of $4^{\bullet+}PF_6^-$ in CH_2Cl_2, EtOH, and CH_3CN; and ESR spectra of $4^{\bullet+}$ at six temperatures between +21 and −90 °C (15 pages). Ordering information is given on any current masthead page.

(22) Nelsen, S. F.; Thompson-Colon, J. A.; Kirste, B.; Rosenhouse, A.; Kaftory, A. *J. Am. Chem. Soc.* **1987**, *109*, 1728.
(23) Nelsen, S. F.; Hintz, P. J. *J. Am. Chem. Soc.* **1972**, *94*, 7108.
(24) Powers, M. J.; Meyer, T. J. *J. Am. Chem. Soc.* **1978**, *100*, 4973.